

Bis-Ruthena(III)cycles $[\text{Ru}(\text{C}^{\wedge}\text{N})_2(\text{N}^{\wedge}\text{N})]\text{PF}_6$ as Low-Potential Mediators for PQQ Alcohol Dehydrogenase ($\text{C}^{\wedge}\text{N} = 2\text{-phenylpyridinato}$ or $4\text{-(2-tolyl)pyridinato}$, $\text{N}^{\wedge}\text{N} = \text{bpy}$ or phen)

Ronan Le Lagadec,^[a] Larissa Alexandrova,^[b] Hebert Estevez,^[a] Michel Pfeffer,^[c] Valdas Laurinavičius,^[d] Julija Razumiene,^[d] and Alexander D. Ryabov*^[e]

Keywords: Ruthenium / Metallacycles / X-ray diffraction / Biosensors / PQQ dehydrogenase

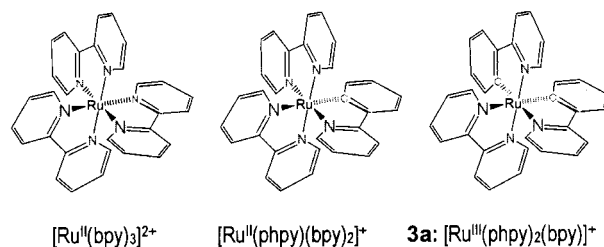
Bis-cyclometalated analogs of tris(2,2'-bipyridine)ruthenium(II), namely $[\text{Ru}^{\text{III}}(\text{C}^{\wedge}\text{N})_2(\text{N}^{\wedge}\text{N})]\text{PF}_6$ complexes **3**, are prepared in 52–57 % yield from the mono-cyclometalated *N,N*-dimethylbenzylamine (dmabH) derivatives $[\text{Ru}^{\text{II}}(\text{dmabH})(\text{N}^{\wedge}\text{N})(\text{MeCN})_2]\text{PF}_6$ ($\text{N}^{\wedge}\text{N} = \text{bpy}$ or phen) and mercurated 2-phenylpyridinato- or 4-(2-tolyl)pyridinato ($\text{C}^{\wedge}\text{N}$) species $\text{Hg}(\text{C}^{\wedge}\text{N})\text{Cl}$. Two new bis-ruthenacycles studied by X-ray crystallography revealed a C_1 symmetry, with the C and N atoms of different $\text{C}^{\wedge}\text{N}$ ligands *trans* to the nitrogen atoms of

the $\text{N}^{\wedge}\text{N}$ ligand. The reduction potential of the $\text{Ru}^{\text{II/III}}$ feature of **3** is as low as ca. –0.2 V (vs. SCE in MeCN). Complexes **3** display a unique mediating ability in moving electrons from the reduced active site of PQQ-dependent alcohol dehydrogenase (PQQ-ADH) to an electrode with 1,2-propanediol as a substrate at a working potential of +0.1 V.

(© Wiley-VCH Verlag GmbH & Co. KGaA, 69451 Weinheim, Germany, 2006)

The $\text{Ru}^{\text{II/III}}$ reduction potential for $[\text{Ru}^{\text{II}}(\text{bpy})_3]^{2+}$ is +1.34 V in MeCN (vs. SCE).^[1] The structurally similar mono-cyclometalated complex $[\text{Ru}^{\text{II}}(\text{phpy})(\text{bpy})_2]^+$ (Scheme 1), in which one N donor is replaced by a σ -bound sp^2 carbon, has a drastically lower $\text{Ru}^{\text{II/III}}$ reduction potential (+0.52 V).^[2] The new bis-cyclometalated species $[\text{Ru}^{\text{III}}(\text{phpy})_2(\text{bpy})]^+$ (**3a**), the central atom of which is σ -bound to two sp^2 carbon atoms, has the lowest $\text{Ru}^{\text{II/III}}$ potentials of ca. –0.2 V. The synthesis, X-ray structural study, and electrochemistry of a new family of Ru^{III} bis-cyclometalated complexes **3** and their record mediating ability in moving electrons from the reduced active site of PQQ-dependent alcohol dehydrogenase (PQQ-ADH) to an electrode are described here. Examples of *bis-cyclometalated Ru complexes* are very limited; those known are the Ru^{II} derivatives of benzo[*h*]quinoline,^[3] azobenzene,^[4] benzylidene aniline,^[5] and $\text{P}(\text{OPh}_3)_3$.^[6] SciFinder tracks the term that is

italicized^[7] but the species listed do not have two Ru–C bonds at one metal center as in **3**.



Scheme 1. A family of related cations discussed in this work. Charges in structures are omitted for clarity.

Two approaches were explored for the synthesis of the blackish-green compounds **3** (Scheme 2). The precursor bis-(acetonitrile) ruthena(II)cycles are cyclometalated 2-phenyl- or 4-(2-tolyl)pyridine (**1**) and *N,N*-dimethylbenzylamine (**2**, dmabH).^[8] Their labile nitrile and dmab ligands are readily substituted in hot methanol by 2-phenylpyridinato or 4-(2-tolyl)pyridinato $\text{C}^{\wedge}\text{N}$ chelates, which are transferred from the corresponding organomercurial compounds **4** or **5**.^[9] Complexes **1** have to be treated with the symmetric organomercurial compound **4**, whereas the reactivity of the asymmetric molecule **5** is sufficient to convert **2** into **3** in 52–57% yield. It is worth noting that the formation of **3** by path **B** resembles the exchange of cyclometalated ligands^[10] at Ru^{II} . Pincer $\text{N}^{\wedge}\text{C}^{\wedge}\text{N}$ ligands were previously replaced by $\text{P}^{\wedge}\text{C}^{\wedge}\text{P}$ fragments at Ru^{II} .^[7c] Path **B** in Scheme 2 illustrates the exchange between bidentate $\text{C}^{\wedge}\text{N}$ chelates.

[a] Instituto de Química, UNAM, Circuito Exterior s/n, Ciudad Universitaria, 04510 Mexico D. F., Mexico

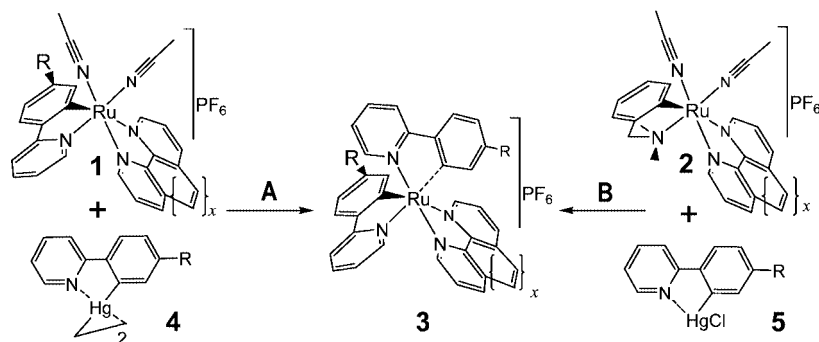
[b] Instituto de Investigaciones en Materiales, UNAM, Circuito Exterior s/n, Ciudad Universitaria, 04510 Mexico D. F., Mexico

[c] Laboratoire de Synthèses Métallo-Induites, UMR CNRS 7513, Université Louis Pasteur, 4 rue Blaise Pascal, 67070 Strasbourg, France

[d] Laboratory of Bioanalysis, Institute of Biochemistry, Mokslininku 12, Vilnius 2600, Lithuania

[e] Department of Chemistry, Carnegie Mellon University, 4400 Fifth Ave., Pittsburgh, PA 15213, USA
E-mail: ryabov@andrew.cmu.edu

Supporting information for this article is available on the WWW under <http://www.eurjic.org> or from the author.



Scheme 2. Syntheses of complexes **3** (a: $x = 0$, R = H; b: $x = 1$, R = H; c: $x = 0$, R = CH₃; d: $x = 1$, R = CH₃).

Two C[∩]N ligands of charge -1 make the complexes susceptible to oxidation, and hence the isolated compounds **3** are paramagnetic Ru^{III} species. Their study by ¹H NMR spectroscopy is complicated, and hence, in addition to the combustion, mass-spectral, and electrochemical analyses, X-ray crystal-structure analysis of **3a** and **3d** was performed. The study on **3a** confirmed its composition (see Supporting Information), but the true stereoisomer (A, B, or C) could not be determined because the three ligands of **3a** are crystallographically identical, and the four nitrogen atoms are indistinguishable from the two carbon atoms.^[11]

The X-ray data for **3d** indicates structure B with C₁ symmetry, which was established by the long Ru–N bond *trans* to the Ru–C σ -bond and by the CH₃ groups at the C[∩]N chelates. There are two different donor atoms, i.e. N and C, *trans* to the nitrogen atoms of the phen ligand in the distorted octahedron. Accordingly, the sp² C1 atom is located *trans* to N21 of the second C[∩]N ligand. The Ru–N21 and Ru–N38 bonds are longer than the other Ru–N bonds, as expected. This reflects the ground state *trans*-influence of the σ -bond sp² atoms C1 and C14, respectively (Figure 1).

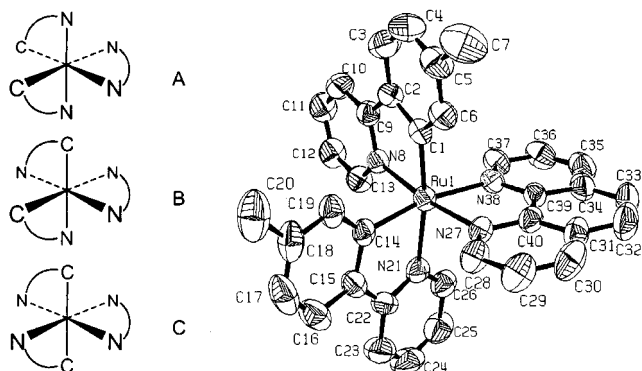


Figure 1. Possible geometric isomers of **3**, A, B, and C, and ORTEP diagram of **3d**. Selected bond lengths: Ru–C1 1.999(3), Ru–N8 2.059(2), Ru–C14 2.0209(3), Ru–N21 2.174(2), Ru–N27 2.067(2), Ru–N38 2.164(2) Å. For X-ray structure of **3a**, see SI.

It is perhaps worth noting that the properties of **3** were previously theoretically investigated.^[12] The bis-ruthenacycles were unknown then, and the calculations were performed for arbitrary selected isomers A and C of C₂ symmetry. Properties of nonexistent species were thus simulated.

Rich cyclic voltammograms of complexes **3** that consist of three one-electron quasi-reversible and one irreversible features (Figure 2, Table 1) were interpreted by using the previously obtained data for mono-cyclometalated species such as [Ru(phpy)(bpy)₂]^{+[2,13]} and [Ru(bpy)₃]^{+[1,14]}. The peaks around -0.2 V represent the Ru^{II/III} couple, since each replacement of bpy by phpy⁻ causes ca. 0.7 V decrease. The peaks at ca. -1.9 and $+1.5$ V could be assigned to the Ru^{I/II} (alternatively, to a ligand-centered reduction) and Ru^{III/IV} couples, respectively. Irreversible peaks at 0.9–1.0 V are presumably due to a ligand-centered oxidation. Post-peaks of lower and variable intensity that follow each peak of **3a** might be due to adsorption; they are not observed for complexes other than **3a**.

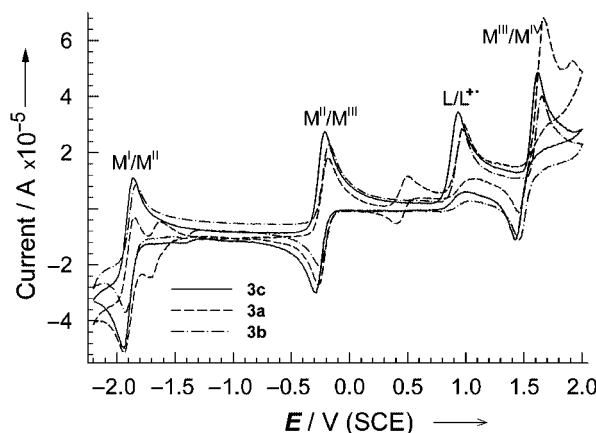


Figure 2. Cyclic voltammograms of ruthena(III)cycles **3** in MeCN (0.1 M *n*Bu₄NPF₆, 0.1 V s⁻¹, 25 °C, glassy carbon, N₂; background subtraction is applied, E₀ = -2.2 V).

Table 1. Assignment of reduction potentials for **3** (in V vs. SCE) from the CVA data in Figure 2 in MeCN.

3	M ^I /M ^{II}	M ^{II} /M ^{III}	L/L ⁺ [a]	M ^{III} /M ^{IV}
3a	-1.90 (-1.67) ^[b]	-0.23 ($+0.45$) ^[b]	0.98	1.56 (1.91) ^[b]
3b	-1.88	-0.21	0.97	1.56
3c	-1.90	-0.25	0.93	1.52

[a] Irreversible. [b] Post-peaks in parenthesis.

The mediating performance of complexes **3**, their precursors **1** and **2**, and related ruthena- and osmacycles in moving electrons from reduced active sites to an electrode^[15] was evaluated with PQQ-ADH (Type II ADH IIG) from

Pseudomonas putida HK5 by using screen-printed carbon paste electrodes.^[16] Remarkably, the largest currents (Figure 3) were registered for the new complexes **3** than for mono-metallated Ru and Os^[17] species, though the optimal electrode potential for **3** was around 0.35 V vs. Ag/AgCl (see Figure S2 of the Supporting Information). Currents in Figure 3 depend hyperbolically on the alcohol concentration ($I = I_{M,app}[S]/(K_{M,app} + [S])$), and the values of $I_{M,app}$ (in parenthesis in Figure 3) emphasize a superior performance of the bis-cycloruthenated species **3**. The major advantage of complexes **3** as mediators of PQQ-ADH is that they are remarkably efficient at a low working electrode potential, i.e. 0.1 V. A decrease in the current because of the voltage drop is minor, and $I_{M,app}$ equals 2290 and 2110 nA for complexes **3a** and **3b**, respectively (cf. with the data in Figure 3).

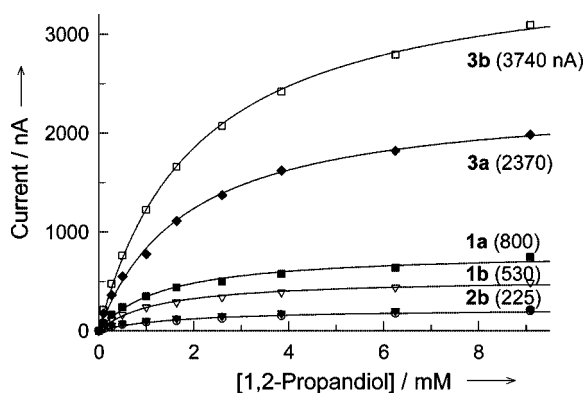


Figure 3. Current as a function of [1,2-propanediol] at 0.5 V for screen-printed electrodes incorporating PQQ-ADH and complexes **1–3**; pH 6, 1 mM Ca²⁺, 22 °C. Numbers in parentheses are calculated values of $I_{M,app}$, which for mono-cyclometalated complexes [Ru(phpy)(phen)(MeCN)₂]⁺X and [Ru(dmiba)(phen)₂]⁺X are close to that of **2b** and for [Os(phpy)(phen)₂]⁺X is that for **1b** (X = PF₆).

In conclusion, the synthesis, full characterization, and numerous properties of previously anticipated but unknown complexes **3** are reported here. The X-ray study of **3d** reveals a structural type B. A “cyclometalation” tool has demonstrated its virtue again by showing how the electronic properties of compositional analogs of [Ru(bpy)₃]²⁺ can further be coarsely altered by replacing N by C donors. An illustrative example of a bioanalytical use of the new complexes **3** highlighted their potential as efficient mediators of enzymatic electron transport which are capable of functioning at low electrode potentials.

Experimental Section

General Procedures for Preparation of [Ru(C[⊖]N)₂(N[⊖]N)]PF₆ (3**) – Path B:** Ru^{II} precursors **1** and **2** were described elsewhere;^[8] **5** and **4** were synthesized according to the procedure of Black et al.^[18] In a Schlenk tube fitted with a condenser, a solution of complex **2** (0.313 mmol) and organomercurial compound **5** (0.313 mmol) in dry methanol (30 mL) was heated at reflux for 20 h. The solvent was evaporated to dryness under vacuum, and the residue was purified by column chromatography on alumina by using a MeCN/CH₂Cl₂ (1:6) mixture as the eluent. The dark green band was col-

lected, and the solvent removed. Blackish crystals were obtained by a slow diffusion of Et₂O into a concentrated solution of the compound in 1:1 MeCN/CH₂Cl₂. Crystals were washed with Et₂O (3 × 10 mL) and dried under vacuum. Reaction of **2** with **4** (Path A) under the same conditions gave compounds **3a–d** in lower yields.

Complex 3a: Yield 52% (115 mg) from 193 mg of **2** and 268 mg of **5**. MS: m/z (%) = 566 (13) [M+H]⁺, 410 (20) [M+H–bpy]⁺, 255 (4) [M+H–bpy–phpy]⁺. IR: 839 (s, PF₆) cm⁻¹. C₃₂H₂₄F₆N₄PRu (711.07): calcd. C 54.09, H 3.40, N 7.88; found C 53.89, H 3.61, N 7.69%.

Complex 3b: Yield 57%. MS: m/z (%) = 590 (100) [M+H]⁺, 436 (23) [M+H–phpy]⁺, 410 (35) [M+H–phen]⁺, 255 (7) [M+H–phen–phpy]⁺. IR: 841 (s, PF₆) cm⁻¹. C₃₄H₂₄F₆N₄PRu (735.07): calcd. C 55.59, H 3.29, N 7.63; found C 55.10, H 3.29, N 7.51%.

Complex 3c: Yield 50%. MS: m/z (%) = 594 (55) [M+H]⁺, 438 (20) [M+H–bpy]⁺, 426 (20) [M+H–tolpy]⁺. IR: 836 (s, PF₆) cm⁻¹. C₃₄H₂₈F₆N₄PRu (739.10): calcd. C 55.29, H 3.82, N 7.59; found C 55.20, H 3.91, N 7.69%.

Complex 3d: Yield 54%. MS: m/z (%) = 618 (65) [M+H]⁺, 450 (10) [M+H–tolpy]⁺, 438 (13) [M+H–phen]⁺. IR: 840 (s, PF₆) cm⁻¹. C₃₆H₂₈F₆N₄PRu·1/2(C₂H₅)₂O (800.13): calcd. C 57.07, H 4.16, N 7.01; found C 56.71, H 4.78, N 6.69%.

Preparation of Biosensors: The screen-printed carbon electrodes (CE) were designed as described.^[16] A carbon paste electrode (working area 0.125 cm²) was impregnated with 4 μL of a solution of mediator **1–3** (1 mg in 1 mL acetone). The enzyme was immobilized on the electrode surface by adsorption of 3 μL of enzyme solution for 1 h. Soluble PQQ-dependent alcohol dehydrogenase (Type II ADH IIG) from *Pseudomonas putida* HK5 (activity 1.54 U/0.2 mL) was used.

Electrochemical Measurements: These were performed with a three-electrode system containing a screen-printed carbon electrode as a working electrode, a Pt wire as a counter electrode, and a saturated KCl Ag/AgCl reference electrode. Steady-state currents were recorded at 0.5 or 0.1 V on a polarographic analyzer PGZ 402 (Radiometer Analytical). Acetate buffer (0.05 M, pH 6.0, 1 mM Ca^{II}) was used. Experimentally measured steady-state currents (I) as a function of the concentration of the substrate of the enzymatic reaction ($[S]$) were fitted to: $I = I_{M,app}[S]/(K_{M,app} + [S])$, where $I_{M,app}$ is the apparent maximal current and $K_{M,app}$ is the apparent Michaelis constant.

Crystallography: The crystals were mounted on the top of glass fibers and transferred to a Bruker SMART-APEX CCD diffractometer. Crystal data and details of data collection and structure refinement are given in Table S1. Absorption corrections were based on face-indexed measurements (program XPREP in SHELXTL).^[19] The structures were refined anisotropically on F^2 with SHELXTL.^[19] For both complexes, hydrogen atoms were included using a riding model. For more details, see Supporting Information. CCDC-606516 and -606515 contain the supplementary crystallographic data for **3a** and **3d**, respectively. These data can be obtained free of charge from The Cambridge Crystallographic Data Centre via www.ccdc.cam.ac.uk/data_request/cif.

Supporting Information (see also the footnote on the first page of this article): Crystal data and structure refinement parameters, details for **3a**, bond lengths and bond angles in Tables S1, S2, and Figure S1; current as a function of applied potential (Figure S2).

Acknowledgments

We thank the University Louis Pasteur for a visiting professorship to A. D. R., Dr. R. A. Toscano for X-ray studies, and CONACyT and the Lithuanian State Science and Studies Foundation (C-02/2005, BIOHEMAS) for support.

- [1] N. E. Tokel-Takvoryan, R. E. Hemingway, A. J. Bard, *J. Am. Chem. Soc.* **1973**, *95*, 6582–6589.
- [2] E. C. Constable, J. M. Holmes, *J. Organomet. Chem.* **1986**, *301*, 203–208.
- [3] J. M. Patrick, A. H. White, M. I. Bruce, M. J. Beatson, D. S. C. Black, G. B. Deacon, N. C. Thomas, *J. Chem. Soc., Dalton Trans.* **1983**, 2121–2123.
- [4] M. I. Bruce, O. B. Shawkataly, M. R. Snow, E. R. T. Tiekink, *Acta Crystallogr., Sect. C* **1987**, *43*, 243–245.
- [5] K. R. Flower, V. J. Howard, R. G. Pritchard, J. E. Warren, *Organometallics* **2002**, *21*, 1184–1189.
- [6] a) M. F. Garbaskas, J. S. Kasper, L. N. Lewis, *J. Organomet. Chem.* **1984**, *276*, 241–248; b) M. I. Bruce, M. R. Snow, E. R. T. Tiekink, *J. Organomet. Chem.* **1986**, *311*, 217–223.
- [7] a) M. Beley, S. Chodorowski, J. P. Collin, J. P. Sauvage, *Tetrahedron Lett.* **1993**, *34*, 2933–2936; b) C. Patoux, J. P. Launay, M. Beley, S. Chodorowski-Kimmes, J. P. Collin, S. James, J. P. Sauvage, *J. Am. Chem. Soc.* **1998**, *120*, 3717–3725; c) P. Dani, M. Albrecht, G. P. M. van Klink, G. van Koten, *Organometallics* **2000**, *19*, 4468–4476; d) P. Dani, M. A. M. Toorneman, G. P. M. van Klink, G. van Koten, *Organometallics* **2000**, *19*, 5287–5296; e) P. Dani, B. Richter, G. P. M. van Klink, G. van Koten, *Eur. J. Inorg. Chem.* **2001**, 125–131.
- [8] a) R. Le Lagadec, L. Rubio, L. Alexandrova, R. A. Toscano, E. V. Ivanova, R. Meškys, V. Laurinavicius, M. Pfeffer, A. D. Ryabov, *J. Organomet. Chem.* **2004**, *689*, 4820–4832; b) A. D. Ryabov, R. Le Lagadec, H. Estevez, R. A. Toscano, S. Hernandez, L. Alexandrova, V. S. Kurova, A. Fischer, C. Sirlin, M. Pfeffer, *Inorg. Chem.* **2005**, *44*, 1626–1634.
- [9] D. S. C. Black, G. B. Deacon, G. L. Edwards, B. M. Gatehouse, *Aust. J. Chem.* **1993**, *46*, 1323–1336.
- [10] A. D. Ryabov in *Perspectives in Coordination Chemistry* (Eds.: A. F. Williams, C. Floriani, A. E. Merbach), Verlag NY, **1992**, pp. 271–292.
- [11] The same was found for [Ru(phpy)(bpy)₂]PF₆: E. V. Ivanova, I. V. Kurnikov, A. Fischer, L. Alexandrova, A. D. Ryabov, *J. Mol. Catal. B: Enzym.*, in press.
- [12] E. C. Constable, C. E. Housecroft, *Polyhedron* **1990**, *9*, 1939–1947.
- [13] a) A. D. Ryabov, V. S. Sukharev, L. Alexandrova, R. Le Lagadec, M. Pfeffer, *Inorg. Chem.* **2001**, *40*, 6529–6532; b) A. D. Ryabov, V. S. Kurova, E. V. Ivanova, R. Le Lagadec, L. Alexandrova, *Anal. Chem.* **2005**, *77*, 1132–1139.
- [14] T.-a. Koizumi, T. Tomon, K. Tanaka, *J. Organomet. Chem.* **2005**, *690*, 1258–1264.
- [15] A. D. Ryabov, *Adv. Inorg. Chem.* **2004**, *55*, 201–270.
- [16] a) J. Razumiene, M. Niculescu, A. Ramanavicius, V. Laurinavicius, E. Csöregi, *Electroanalysis* **2002**, *14*, 43–49; b) V. Laurinavicius, J. Razumiene, A. Ramanavicius, A. D. Ryabov, *Bio-sens. Bioelectron.* **2004**, *20*, 1217–1222.
- [17] A. D. Ryabov, V. S. Soukharev, L. Alexandrova, R. Le Lagadec, M. Pfeffer, *Inorg. Chem.* **2003**, *42*, 6598–6600.
- [18] D. S. C. Black, G. B. Deacon, G. L. Edwards, B. M. Gatehouse, *Aust. J. Chem.* **1993**, *46*, 1323–1336.
- [19] G. M. Sheldrick, *SHELXTL* (Version 6.10), Bruker AXS Inc., Madison, Wisconsin, USA, **2000**.

Received: March 10, 2006
Published Online: June 7, 2006